



Open Research Online

The Open University's repository of research publications and other research outputs

In-situ nanoSIMS measurements of isotopic hotspots in the CM2 meteorite Cold Bokkeveld

Conference or Workshop Item

How to cite:

Snape, J. F.; Morlock, A.; Starkey, N. A.; Franchi, I. A. and Gilmour, I. (2013). In-situ nanoSIMS measurements of isotopic hotspots in the CM2 meteorite Cold Bokkeveld. In: 44th Lunar and Planetary Science Conference, 18-22 Mar 2013, The Woodlands, TX, USA, p. 1913.

For guidance on citations see [FAQs](#).

© 2013 The Authors

Version: Version of Record

Link(s) to article on publisher's website:

<http://www.lpi.usra.edu/meetings/lpsc2013/pdf/1913.pdf>

Copyright and Moral Rights for the articles on this site are retained by the individual authors and/or other copyright owners. For more information on Open Research Online's data [policy](#) on reuse of materials please consult the policies page.

oro.open.ac.uk

IN-SITU NANOSIMS MEASUREMENTS OF ISOTOPIC HOTSPOTS IN THE CM2 METEORITE COLD BOKKEVELD. J. F. Snape¹, A. Morlok^{1,2}, N. A. Starkey¹, I. A. Franchi¹ and I. Gilmour¹, ¹Planetary and Space Sciences, The Open University, Milton Keynes, MK7 6AA, U.K. (joshua.snape@open.ac.uk), ²Institut für Planetologie, Wilhelm-Klem-Str. 10, Münster, Germany.

Introduction: Previous studies have identified isotopic hotspots in insoluble organic matter (IOM) from carbonaceous chondrites [e.g. 1,2]. The origins and formation mechanisms of these hotspots and the host IOM are a matter of ongoing debate. For example, it is not clear whether D and ¹⁵N enrichments in IOM formed within a common organic precursor in cold interstellar environments [3,4] or due to irradiation of organic material in the early Solar System [5,6]. It is also unclear what effect parent body processes would have had with regard to the alteration of meteoritic IOM [2]. In order to address these issues, more recent studies have attempted to make in-situ measurements of isotopic anomalies in IOM [e.g. 5]. In this study we present in-situ NanoSIMS isotopic analyses of material within a sample of the CM2 meteorite Cold Bokkeveld, comparing the distribution of hotspots and bulk H, C and N isotopic composition in the rims and interiors of altered chondrules.

Analytical Techniques: Back scattered electron (BSE) images were acquired with an FEI Quanta 200 3D microscope. These were then used to identify regions of interest within the sample (Fig. 1). C, N and H isotopic ratios were determined using a Cameca NanoSIMS 50L. Areas of 30×30 μm² were extensively pre-sputtered with the ion beam. Within these areas, 25×25 μm² regions were mapped with two different analytical setups: (1) ¹²C, ¹³C, ¹⁶O, ¹⁸O, ¹²C¹⁴N, ¹²C¹⁵N

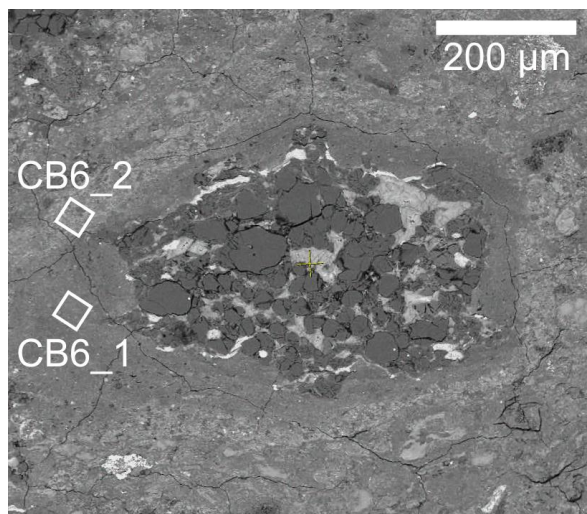


Figure 1. BSE image of a chondrule (CB6) in Cold Bokkeveld. Areas analysed by NanoSIMS have been indicated with white squares.

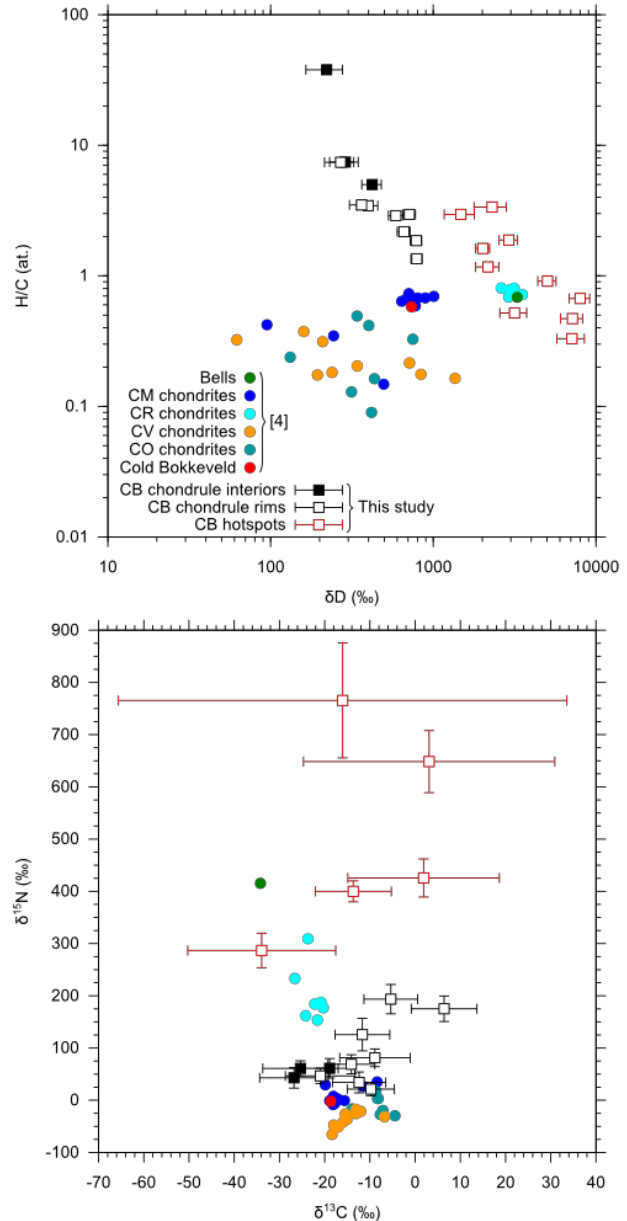


Figure 2. (a) δD vs. H/C and (b) $\delta^{13}C$ vs. $\delta^{15}N$ values for areas within Cold Bokkeveld. Data are compared with those of IOM from other carbonaceous chondrites [4]. Filled symbols represent analyses within chondrules, open symbols represent analyses of chondrule rim material.

(4 pA probe, MRP >9000); and (2) ¹H, ²H, ¹²C and ¹⁸O (10pA, MRP ≈ 4000). Data were reduced using the L'Image software (L. Nittler, Carnegie Institution of Washington). Post-NanoSIMS secondary electron (SE) images were acquired using a Zeiss Supra 55V

analytical FEG SEM (Fig. 3a). All of the hotspots identified have sigma values of >4 (as calculated in L'Image).

Results: A total of thirteen areas were analysed within three separate chondrules and their rims. An example of one such chondrule (CB6) is presented in Fig. 1. The bulk δD , $\delta^{15}N$ and $\delta^{13}C$ isotopic compositions of these areas are within the range reported for IOM in other carbonaceous chondrites (Fig. 2; [4]). H/C ratios within the Cold Bokkeveld areas are significantly higher than those of carbonaceous chondrite IOM, however, this is almost certainly due to the fact that these areas also include non-organic phyllosilicate material. The highest bulk δD , $\delta^{15}N$ and $\delta^{13}C$ values are observed within the rims of chondrules while the highest H/C ratios are observed in the chondrule interiors (Fig. 2).

D-enrichments. D-enrichments are identified in the rims of several chondrules (Fig. 2a). CB6_2 is an example of one area within which multiple D-enrichments were observed (Fig. 3c-d). These appear to correspond to depressions in the surface of the sample, as indicated in the SE image of CB6_2 (Fig. 3a). The D-enrichments also correlate to relatively C-rich areas of the sample (Fig. 3b).

^{15}N -enrichments. Less common than the D-enrichments are ^{15}N hotspots. However, one area within the rim of a chondrule (CB6_2) was found to contain several such hotspots (Fig. 2b). All of these corre-

spond to relatively C-rich areas and two correspond to D-enrichments (Fig. 3c-f).

Discussion: The variation of bulk δD values might reflect the incorporation of multiple materials into the chondrules [5], or could be due to post-accretionary remobilisation of D-rich IOM [2]. As with previous studies, our results indicate that ^{15}N and D hotspots are not always spatially correlated [1,3]. Based on the models of [3], nitriles are the most likely source of the ^{15}N -enrichments that do not appear to be correlated with D hotspots. The combined ^{15}N - and D-enrichments are most likely carried by amines. The putative association observed between isotopically anomalous IOM and chondrule rims and altered matrix may indicate the remobilisation of D-rich IOM post accretion. More detailed characterisation of the mineralogical environment of D-rich grains may assist in establishing the extent to which equilibration of D has, or has not, occurred on parent bodies.

Acknowledgments: We thank Gordon Imlach from the electron microscope suite at the Open University for his assistance in the acquisition of SE images.

References: [1] Busemann H. et al. (2006) *Science*, 312, 727–730. [2] Alexander C. M. O'D. et al. (2010) *GCA*, 74, 4417–4437. [3] Wirström E. S. et al. (2012) *ApJ*, 757, L11. [4] Alexander C. M. O'D. et al. (2007) *GCA*, 71, 4380–4403. [5] Remusat L. et al. (2010) *ApJ*, 713, 1048–1058. [6] Aleon J. (2010) *ApJ*, 722, 1342–1351.

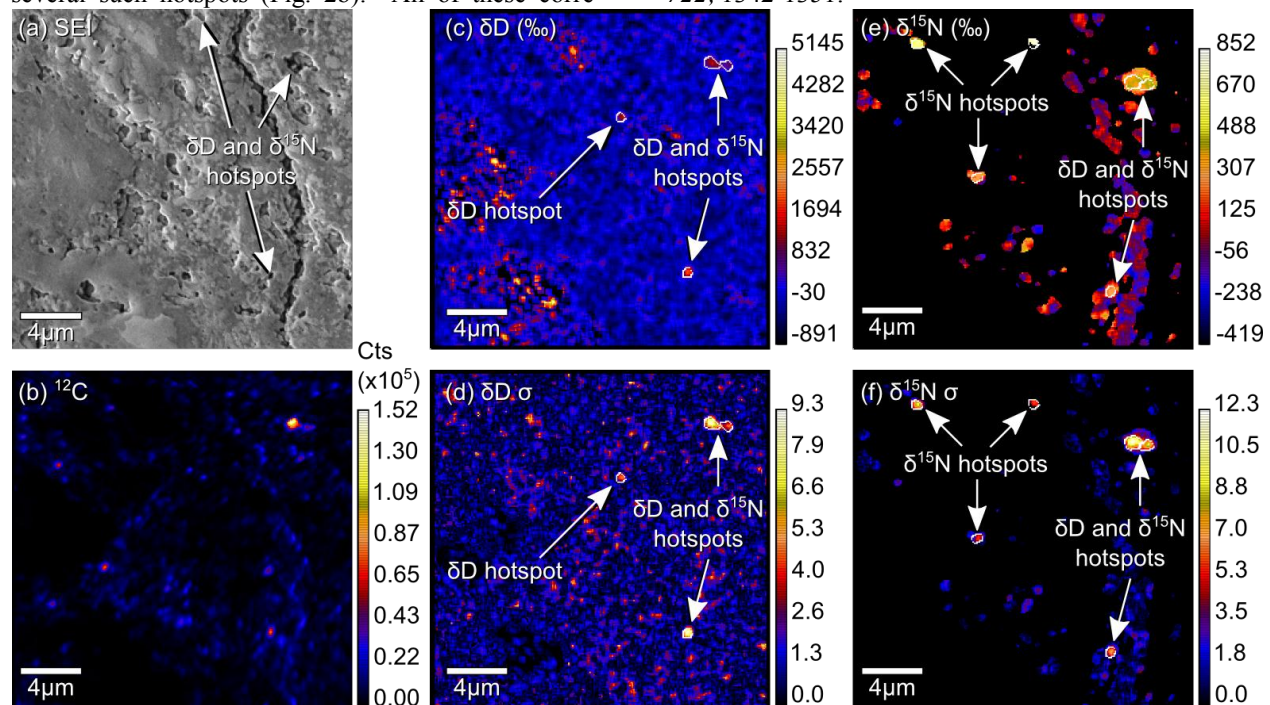


Figure 3. (a) SE image of analysed area CB6_2 with the locations of isotopic hotspots indicated. (b) NanoSIMS map illustrating ^{12}C concentration within CB6_2. (c) δD variations within CB6_2 and associated δD σ map (d). (e) $\delta^{15}N$ variations within CB6_2 and associated $\delta^{15}N$ σ map (f).